

Role of subtropical Rossby waves in governing the track of cyclones in the Bay of Bengal

**Vineet Kumar Singh<sup>1,2</sup>, M.K. Roxy<sup>1</sup> and Medha Deshpande<sup>1</sup>**

<sup>1</sup> Indian Institute of Tropical Meteorology, Ministry of Earth Sciences, Pune, India

<sup>2</sup> Department of Atmospheric and Space Sciences, Savitribai Phule Pune University, Pune, India

Corresponding author: Vineet Kumar Singh ([vineetsingh.jrf@tropmet.res.in](mailto:vineetsingh.jrf@tropmet.res.in))

**Key points:**

- Cyclones during November in the Bay of Bengal follow two distinct tracks: west-northwestward and north-northeastward tracks.
- A Rossby wave train originating from East Atlantic/Mediterranean region governs the upper-level winds over the Indian subcontinent.
- Presence of subtropical Rossby wave train steers the cyclone north-northeastwards and in its absence, cyclone moves west-northwestwards.

**Abstract**

The cyclones during November in the Bay of Bengal follow two distinct tracks. Some cyclones move west-northwestward and make landfall at Odisha, Andhra Pradesh, Tamil Nadu or Sri Lanka coast while others move north-northeastwards and make landfall at West Bengal, Bangladesh or Myanmar coast. We found that there is a difference in the steering winds governing these two different cyclone tracks. The north-northeastward moving cyclones are associated with an anomalous upper-level cyclonic circulation over India which is a part of a sub-tropical wave train. This wave train is triggered by an anomalous upper-level convergence over the Mediterranean region near the subtropical westerly jet entrance. The jet acts as a Rossby waveguide and excites an eastward propagating wave train which propagates from the East Atlantic/Mediterranean region and reaches the Indian subcontinent in four days. This wave train induces an anomalous cyclonic circulation over Indian landmass and provides south-to-north and west-to-east steering over the Bay of Bengal causing the cyclones to move in a north-northeastward direction. On the other hand, for west-northward moving cyclones, there is no Rossby wave intrusion over the Indian subcontinent, hence the cyclones move in west-northwestward direction assisted by the climatological winds which are from east to west over the south and central Bay of Bengal. This shows that the track of the cyclone in the north Indian Ocean can be modulated by the atmospheric changes in the extratropics and can act as a precursor for the prediction of the track of the cyclone in this region.

**Plain language Summary**

Cyclones in the Bay of Bengal during November follow two different tracks. Some cyclones move west-northwestward and make landfall at the Odisha, Andhra Pradesh, Tamil Nadu or Sri Lanka coast while others move north-northeastwards and make landfall at the West Bengal, Bangladesh, or Myanmar coast. For the period 1982–2019, we find that there is a significant difference in the upper-level (300 hPa) winds that prevail over the Indian sub-continent during these two distinct cyclone tracks. These upper-level winds that govern the tracks of cyclones in the Bay of Bengal are modulated by atmospheric disturbances in higher latitudes which propagate eastward as a wave towards India. These atmospheric waves originate over the East Atlantic/Mediterranean region and reach the Indian subcontinent in four days. The eastward propagation of these atmospheric waves result in southerly and westerly winds over the Bay of Bengal leading to cyclones moving in a north-northeast direction. On the other hand, for the west-northwestward moving cyclones, there is an absence of eastward-moving atmospheric waves. Hence the cyclones follow the climatological winds which are from east to west in south and central Bay of Bengal causing the cyclones to move in a west-northwest direction.

**Keywords:** tropical cyclone, cyclone track, Bay of Bengal, Rossby wave

## 1. Introduction

The north Indian Ocean, including the Bay of Bengal and the Arabian Sea, has two cyclone seasons in a year, the pre-monsoon season during April–June and the post-monsoon season during October–December (Li et al., 2013). The post-monsoon season is the primary cyclone season with a higher frequency of cyclones as compared to the pre-monsoon season (Li et al., 2013). The frequency of the cyclones in the Bay of Bengal is more as compared to the Arabian Sea (Alam et al., 2003; Sahoo & Bhaskaran, 2016; Singh et al., 2019; Singh & Roxy, 2020). The north Indian Ocean accounts for only 6% of the global annual cyclone frequency (Singh & Roxy, 2020). Despite the less number of cyclones as compared to other basins, extremely severe cyclones form in the Bay of Bengal that cause extensive casualties in the Bay of Bengal rim countries including India, Bangladesh and Myanmar (Chittibabu et al., 2004; Kikuchi et al., 2009; Lin et al., 2009; Madsen & Jakobsen, 2004; Yanase et al., 2010). Not only the fatalities but also the economic loss due to these cyclones is huge. Cyclone Amphan, which hit the West Bengal coast in May 2020, was the costliest north Indian Ocean cyclone on record with an estimated loss of US\$ 14 billion (WMO, 2021).

Multiple large-scale factors govern the cyclogenesis and intensification of the cyclone in the Bay of Bengal. It is seen that El Niño Southern Oscillation (ENSO) significantly modulate the cyclone activity in this basin with La Niña favouring more cyclogenesis and intense cyclones as compared to the El Niño (Balaguru et al., 2016; Bhardwaj et al., 2019; Felton et al., 2013; Girishkumar et al., 2015; Girishkumar & Ravichandran, 2012; Mahala et al., 2015; Mohapatra & Vijay Kumar, 2017; Ng & Chan, 2012). Also, negative Indian Ocean Dipole enhances the cyclone frequency in this basin and positive Indian Ocean Dipole suppresses

it (Biswas & Kundu, 2018; Girishkumar & Ravichandran, 2012; Mahala et al., 2015; Mohapatra & Vijay Kumar, 2017). Further, the active phase of Madden Julian Oscillation enhances the probability of cyclogenesis and provides conducive conditions for rapid intensification (Krishnamohan et al., 2012; Singh et al., 2020; Singh et al., 2021). However, we still lack an in-depth understanding of the effect of the changes in the large-scale atmospheric winds that can affect the track of the cyclone in the Bay of Bengal.

The track of the cyclone is generally controlled by three factors. First is the beta drift which steers the cyclone in the northwest direction in the northern hemisphere due to the gradient of absolute vorticity (Johnny C.L. Chan, 2005; Johny C. L. Chan & Williams, 1987; Williams & Chan, 1994). Second is the asymmetry in the convection which is governed by the sea surface temperature (SST) gradient (DeCaria 2005). The asymmetrical convection can cause a decrease of mean sea level pressure in the eye of the cyclone, which can lead to movement of the eye of the cyclone in the direction of the mean sea level pressure. The third factor is the background winds which steer the cyclone in their direction (George & Gray, 1976; L. Wu & Wang, 2004). It is seen that out of these three factors, the dominant factor that controls the track of the cyclone is the background steering winds (Holland, 1983; Wang et al., 1998; L. Wu & Wang, 2004; Yun et al., 2012). The winds in the upper level play a dominant role in steering the cyclone (Chan & Gray, 1982; Neumann, 1993; Singh et al., 2020; Srinivasan & Ramamurthy, 1973). These steering winds during the time of the cyclone are controlled by a large number of factors depending on the ocean basin, the month of the year, prevailing climate mode of variability and the atmospheric waves.

In the Atlantic Ocean, it is observed that the ENSO and the North Atlantic Oscillation significantly alters the track of the cyclones by changing the steering winds (Elsner, 2003; Kossin et al., 2010; Mei et al., 2014; Xie et al., 2005). In the Northwest Pacific it is observed that ENSO, Pacific Decadal Oscillation, monsoon trough, the position and the strength of western North Pacific subtropical high-pressure area governs the track of the cyclones in this basin (Chen et al., 2009; Harr & Elsberry, 1991; Ho et al., 2004; Ko & Hsu, 2006; Liu & Chan, 2008; Liguang Wu et al., 2005; Q. Wu et al., 2020; Zhang et al., 2012, 2013). In the north Indian Ocean, the Indian Ocean Dipole modulates the winds in the lower level with westerly wind anomalies during the positive Indian Ocean Dipole year in the central Bay of Bengal that prevents the westwards movement of the cyclone (Mahala et al., 2015; Yuan & Cao, 2013). During the negative Indian Ocean Dipole years, there are anomalous easterlies in the central Bay of Bengal that lead to more westward-moving cyclones in this region (Yuan & Cao, 2013). For the period 1993–2010, Girishkumar and Ravichandran (2012) show that, during a La Niña, the upper level winds (200 hPa) are from southeast to north-northwest direction in the Bay of Bengal and the genesis of the cyclone in the post-monsoon season is mainly in the east Bay of Bengal. as a result, the 200 hPa winds steer the cyclones in northwest-north direction. However, during El Niños, the genesis location of the cyclone is in the west Bay of Bengal

and as a result the cyclone makes landfall quickly after their genesis without getting significantly affected by the steering winds at the 200 hPa (Girishkumar & Ravichandran, 2012). These studies for the north Indian Ocean focus only on the seasonal time scale to study the factors controlling the track of the cyclones in the Bay of Bengal. However, it is observed that in some years cyclones follow different tracks during the same season. This shows that intraseasonal variability also plays a dominant role in altering the wind circulation over the Bay of Bengal which in turn can affect the track of cyclones.

It is observed that the perturbations in the sub-tropical westerly jet significantly alters the wind circulation pattern at intraseasonal time scale in the upper level all along the jet axis from the Mediterranean region to southeast China and Japan including the Indian subcontinent (Bo-Tao, 2013; Ding & Li, 2017; Li & Sun, 2015; Li et al., 2017a; Syed et al., 2006; Wen et al., 2009; Yang et al., 2004; Zhou et al., 2009). In boreal winter, the jet is anchored at 25°N over North Africa and East Asia. Studies show the role of the westerly jet in carrying the upstream perturbations in the atmospheric circulation over the Atlantic and adjoining Mediterranean region to the downstream regions via Rossby wave propagation along the jet (Li & Sun, 2015; Song et al., 2014; Watanabe, 2004; Xiuzhen & Zhou, 2016). The jet act as a waveguide for the downstream propagation of stationary Rossby waves (Branstator, 2002; Hoskins & Ambrizzi, 1993). This meridionally trapped and zonally elongated wave train along the axis of the jet in the upper level is also called as South Asia jet wave train (Huang et al., 2020). The South Asia jet wave train propagation is observed at multiple time scales such as synoptic timescales (Li & Sun, 2015; Li et al., 2017b), intraseasonal time scales (Miaoqing et al., 2008; Ren et al., 2015) and interannual timescales (Watanabe, 2004). The source of this wave train is found to be the perturbations caused by the North Atlantic Oscillation in the Atlantic Ocean and the upper-level convergence over the Mediterranean Sea near the jet entrance region over South Asia (Ding & Li, 2017; C. Li & Sun, 2015; Song et al., 2014; Watanabe, 2004).

Over the Indian subcontinent using the reanalysis data, Yang et al. (2004) show that the strength and the location of the sub-tropical westerly jet significantly alter the monsoon circulation. For the period 1979–2003, Ding and Wang (2007) show that the eastward and southward propagation of the wave train originating from the northeastern Atlantic plays a prominent role in the intraseasonal variability of the southwest monsoon over the Indian region. Based on the reanalysis dataset for the period 1958–2016, Li et al. (2020) interpreted that the changes in the atmospheric circulation due to the ocean-atmosphere interaction in the north Atlantic propagates to the Indian region via the waveguide effect of the subtropical westerly jet stream and leads to the variability in the southwest monsoon circulation. Not only the southwest monsoon but also the winter precipitation in northwest India adjoining Pakistan and Iran is altered by the Rossby wave propagation in the upper level along the sub-tropical westerly jet (Hunt et al., 2018a,b; Syed et al., 2006). This Rossby wave propagation from the northwest Africa/Mediterranean to the Indian region along the South Asia

jet axis is also called as a western disturbance (Miaoqing et al., 2008; Syed et al., 2006).

From the above-mentioned studies, it is seen that the Rossby wave propagation along the subtropical westerly jet significantly modulates the atmospheric circulation and weather over Asia including India in different seasons. This shows that intraseasonal oscillation might be playing a crucial role in changing the winds at upper levels over the Indian subcontinent and determining the track of the cyclone in the Bay of Bengal. Hence, our main objective in this study is to understand the influence of the intraseasonal variability governing the track of the cyclones in the Bay of Bengal during the post-monsoon season (November).

## 2. Data and Methodology

We analyze the factors controlling the track of cyclones in the Bay of Bengal that formed in November during the period 1982–2019. The cyclone data is taken from 1982 onwards as from this time there is an improved network of ocean observations and better satellite observations are available (Landsea, 2005). The cyclone data for the above-mentioned period is obtained from the International Best Track Archive for Climate Stewardship (IBTrACS) cyclone dataset (Knapp et al., 2010). Daily data of various atmospheric parameters are obtained from the ERA5 reanalysis dataset provided by European Centre for Medium-Range Weather Forecasts (ECMWF). Daily anomalies of various atmospheric parameters are computed based on daily climatology for the period 1982–2019.

In the post-monsoon season (October–December), only November is chosen for analysis as in this month the cyclones follow two distinct tracks (Figure 1). One cluster of cyclones follows the west-northwest track, make landfall over the Tamil Nadu, Andhra Pradesh or Odisha coasts of India or Sri Lanka (henceforth west-northwestward moving cyclones). The other cluster of cyclones follows the north-northeastwards track, make landfall over the West Bengal coast of India, Bangladesh or Myanmar (henceforth north-northeastward moving cyclones). In October and December, the north-northeastward moving cyclones are negligible as compared to the west-northwestward moving cyclones, therefore the cyclones which form in these two months are not included in the current analysis.

To understand the difference in the wind pattern over the Indian subcontinent during the north-northeastward and west-northwestward moving cyclone, we removed the cyclone vortex from the winds so that the influence of cyclone winds on the background steering winds is minimal in the analysis. The removal of cyclone vortex is based on the method devised by Galarneau and Davis (2013). In this method, they separate the winds into the cyclone and non-cyclone wind components. The cyclone components of stream function and velocity potential are defined by equations 1 and 2

$$\begin{aligned}\nabla^2\psi &= \xi, \quad (r \leq r') \text{ Equation 1} \\ &= 0, \quad (r \geq r')\end{aligned}$$

$$\nabla^2\chi = \delta, (r \leq r') \text{ Equation 2}$$

$$= 0, (r \geq r')$$

Where  $\chi$  is the stream function,  $\delta$  is the relative vorticity,  $\psi$  is the velocity potential and  $\nabla$  is the divergence,  $r$  is the radius of the cyclone. From the above equation, cyclone-related rotational and divergent wind components are estimated using the cyclone-related stream function and velocity potential, respectively. Using this method, all the divergent and rotational wind components associated with the cyclone is removed from the wind and only the background wind is left. To understand the synoptic evolution of atmospheric features that govern the tracks of the cyclones in the Bay of Bengal in November month, a lead-lag analysis is carried out. For the lead-lag analysis, day 0 is the day when the cyclone has its genesis as per the cyclone data available from the IBTrACS dataset. We have taken genesis day as the day when the system has attained a wind speed of 20 knots. We use this threshold for genesis as for some cyclones, wind speed less than 20 knots is not reported in the IBTrACS dataset. Similarly, day -1, day -2 and so on are the days before the cyclone genesis and day +1, day +2 and so on are the days after the cyclone genesis. Generally, the winds at the upper level (200-300 hPa) control the steering of the cyclones (Neumann, 1993; Pattanaik & Rama Rao, 2009). To extract the dominant mode of variability in the winds at the upper level in November over the Indian subcontinent (40°-120°E, 10°-40°N), an empirical orthogonal function (EOF) analysis of the daily meridional wind anomalies at 300 hPa is performed.

Daily time-longitude cross-sections (averaged over 20°-35°N) of regressed meridional wind, geopotential height and divergence anomalies at 300 hPa were analyzed to see the evolution and propagation of the Rossby wave along the subtropical westerly jet. Statistical significances of the daily anomalies obtained from linear regression are estimated according to a two-tailed Student's  $t$  test.

### 3. Results

#### 3.1. Atmospheric circulation during west-northwestward moving and north-northeastward moving cyclone

During the period 1982–2019, 34 cyclones formed in the Bay of Bengal in November that made landfall at the Bay of Bengal rim countries. Out of these 34 cyclones, 9 were north-northeastward moving that made landfall at the West Bengal, Bangladesh or Myanmar coasts (Figure 1). The remaining 25 cyclones were west-northwestward moving that made landfall at Sri Lanka, Tamil Nadu, Andhra Pradesh or Odisha coasts (Figure 1). In the northwest Pacific Ocean, the genesis location of the cyclone is found to determine the track of the cyclone in a west-northwest direction or recurving in a northeast direction (Yonekura & Hall, 2014). Hence, to see whether in the Bay of Bengal also, the two types of cyclone track clusters are influenced by the genesis location of the cyclone, we computed the average genesis location of the cyclones in these two track clusters. It is observed that the average genesis location of the north-northeastward moving cyclones is 10.5°N, 93.4°E, whereas, the average genesis location of the

west-northwestward moving cyclone is  $9.8^{\circ}\text{N}$ ,  $91.1^{\circ}\text{E}$ . Using the two-tailed Student's  $t$  test, we found that there is no statistically significant difference at 95% confidence level between the genesis locations of these two cyclone track clusters. This shows that the genesis locations of these two clusters of cyclone track is not playing a crucial role in governing the different landfall locations of the cyclones.

Studies show that the cyclones are generally steered by the upper-level background atmospheric winds (Pattanaik & Rama Rao, 2009; Srinivasan & Ramamurthy, 1973; L. Wu & Wang, 2004). The climatological winds at the upper level (300 hPa) in November is shown in Figure S1. It can be seen from Figure S1, that as per the climatology easterly winds prevail over the south Bay of Bengal up to  $10^{\circ}\text{N}$  and southeasterlies winds are there over the central Bay of Bengal around  $10^{\circ}$ - $15^{\circ}\text{N}$ . In order to understand the difference in the atmospheric background wind pattern between the two clusters of cyclone tracks, we analyzed the composite of actual upper-level winds and upper level wind anomalies (300 hPa) after removing the cyclone vortex from the winds (Figure 2a-h). During 1982–2019, the average lifespan of the cyclones in the Bay of Bengal in November is six days. So, we analyzed the daily evolution of the composite of the 300 hPa actual winds and the wind anomalies from day 0 till day +6 for the two cyclone track clusters over the region  $40^{\circ}$ - $120^{\circ}\text{E}$ ,  $0$ - $40^{\circ}\text{N}$ , where day 0 is the day when the cyclone has its genesis, day +1 is 1 day after the genesis of the cyclone, and so on. However, we show the composite evolution of wind and wind anomalies only for selected days in Figure 2. It is seen from Figure 2a-d that there is a difference in the upper-level winds governing the two clusters of cyclone tracks. For the north-northeastward moving cyclones on day 0 and day +4, the subtropical westerlies penetrate more southwards (up to  $16^{\circ}\text{N}$ ) over the Indian landmass and the western Bay of Bengal as compared to the climatology (Figure 2a and 2c). Also, over the central Bay of Bengal the winds are from south to north. On the other hand, for the west-northwestward moving cyclones, the westerlies are restricted up to  $20^{\circ}\text{N}$ , and over the central Bay of Bengal the south to north winds are weak (Figure 2b and 2d). In order to show the difference in the winds between these two composites we analyzed the upper-level (300 hPa) wind anomalies. For the north-northeastward moving cyclones, on day 0, there are anomalous southerlies over central and north Bay of Bengal (Figure 2e). On day +2, there are anomalous southerlies in the north Bay of Bengal and anomalous westerlies over the central and south Bay of Bengal (Figure not shown). On day +4 and day +6 also, there are anomalous southerlies over the north and the central Bay of Bengal and anomalous westerlies over the remaining parts of the basin (Figure 2g). These wind anomalies from day 0 to day +6 are associated with an anomalous cyclonic circulation centered over India landmass at around  $75^{\circ}$ - $80^{\circ}\text{E}$ . Also, it can be seen that there are two anticyclonic wind anomalies east and west of India centered over  $110^{\circ}\text{E}$ ,  $25^{\circ}$ - $30^{\circ}\text{N}$  and  $45^{\circ}\text{E}$ ,  $25^{\circ}$ - $30^{\circ}\text{N}$  respectively (Figure 2e, g). This chain of cyclonic and anticyclonic circulations from the Arabian Peninsula to east China are in the path of the climatological position of the subtropical westerly jet (Kuang &

Zhang, 2005). These circulation anomalies give an indication of a wave pattern in the upper-level atmospheric winds along the path of the subtropical westerly jet. That is leading to the development of anomalous cyclonic circulation over India and steering the cyclones in the north-northeastward direction.

For the west-northwestward moving cyclones, it is seen that from day 0 to day +6 there are anomalous easterlies at the upper-level over most parts of the Bay of Bengal (Figure 2f, h). There is an absence of anomalous cyclonic circulation over India landmass as seen in the case of the composites of the north-northeastward moving cyclones. Also, the anticyclonic circulation over the Arabian Peninsula and east China is absent. Due to the absence of wave-like features in the upper-level winds which is observed in the composites of north-northeastward moving cyclones and anomalous easterlies over the Bay of Bengal, the cyclones move in a west-northwestward direction.

Studies have shown earlier that the presence of anomalous cyclonic and anticyclonic circulation over the Indian subcontinent along the subtropical westerly jet axis is associated with an eastward-moving Rossby wave along the jet axis (Li & Sun, 2015; Song et al., 2014; Sun et al., 2018). To see whether the different atmospheric wind patterns over the Indian region during the two cyclone track clusters are associated with the changes in large scale atmospheric circulation pattern, we have analyzed the daily composite evolution of the upper-level meridional wind anomalies from day -10 to day +6 over the Indo-Atlantic tropical and extratropical regions for these clusters. The composite evolution is shown in Figure 3, though only for selected days. Meridional winds are best suited to study the propagation of atmospheric waves in the upper levels (Wirth et al., 2018). Figure 3a-c shows the composite evolution of meridional wind anomalies for the north-northeastward moving cyclones. It can be seen that at day -4, there are anomalous southerly winds over the east-central Atlantic Ocean near 40°N, penetration of northerly winds from west Europe up to north Africa and again southerly wind anomalies are seen over the eastern Mediterranean region. This forms an anomalous anticyclonic circulation over the east Atlantic/western Mediterranean region and anomalous cyclonic circulation over the east-central Mediterranean region. By day -2, alternating southerly and northerly winds are seen extending up to the Arabian Sea as seen from northerly wind anomalies over the north Arabian at around 60°E. At day 0, the alternating southerly and northerly propagates eastward up to the Bay of Bengal with anomalous southerly winds developing over the north Bay of Bengal and anomalous cyclonic circulation is established over the Indian landmass. This anomalous cyclonic circulation and the associated southerly wind anomalies over the Bay of Bengal steers the cyclone in the north-northeastward direction. Composite daily evolution of meridional winds for the west-northwestward moving cyclone (Figure 3d-f) shows that before the cyclone formation (day 0) there is an absence of anomalous alternating southerly and northerly winds from west Mediterranean/eastern Atlantic to the Bay of Bengal along the subtropical westerly jet axis as seen during the north-northeastward moving cyclones. Due to the lack of external subtropical forcing the cyclone follow a north-northwestward track.

### 3.2. Role of Rossby wave propagation in altering the wind circulation over India

It is seen that in the case of the north-northeastward moving cyclones, the anomalous alternating southerly and northerly wind anomalies from the subtropical eastern Atlantic to the Bay of Bengal, are along the subtropical westerly jet axis. Earlier studies show that the upper-level disturbance at the jet entrance region (Mediterranean region) is propagated downstream towards east China in the form of a Rossby wave train along the subtropical westerly jet axis (Miaoqing et al., 2008; Watanabe, 2004). The Rossby wave train induces alternating anomalous convergence and divergence zone along the jet axis (Miaoqing et al., 2008). The subtropical westerly jet thus provides a favourable waveguide for the propagation of Rossby wave along the jet axis (Branstator, 2002).

To see whether the anomalous wind pattern during the north-northeastward moving cyclones is connected with the zonal eastward propagation of the Rossby wave train, we have done an EOF analysis on the daily meridional wind anomaly at 300 hPa in November for the period 1982–2019. For the EOF analysis, we selected the region  $40^{\circ}$ – $120^{\circ}$ E,  $10^{\circ}$ – $40^{\circ}$ N as the changes in the winds in this region have a direct effect on the track of cyclones in the Bay of Bengal. Li et al. (2017b) show that even focusing on only one of the active centers of the wave, the entire zonal propagation of the Rossby wave can be analyzed. We found that the first and second EOF mode accounts for 22.5% and 20.92% of the total variance respectively. The remaining modes have very little variance as compared to the first two modes. From Figure 4a, b it can be seen that both the EOF modes feature a wave train with anomalous southerly and northerly winds illustrating anomalous cyclonic and anticyclonic circulations along the jet axis centered at around  $30^{\circ}$ N. This feature is similar to those documented in the previous studies (Hu et al., 2018; Huang et al., 2020). In the first mode of EOF (EOF1), there are anomalous northerlies over the north Arabian Sea and anomalous southerlies over the north Bay of Bengal (Figure 4a). In the second mode of EOF (EOF2), there is a shift in the activity centers with anomalous southerly over the India landmass and anomalous northerly west and east of it centered at around  $50^{\circ}$ E and  $110^{\circ}$ E respectively (Figure 4b). Huang et al. (2020) show that these first two modes of EOFs represent the same wave train along the subtropical westerly jet stream axis in different phases. The pattern in EOF1 resembles the composites of north-northeastward moving cyclones. Since EOF1 is the leading mode with a variance of 22.5% and its positive pattern resembles the wind pattern in north-northeastward moving cyclones, we use it for the rest of the analysis.

We further use the lead-lag regression of various atmospheric variables onto the first principal component (PC1) of EOF1 to study the evolution and the propagation of the wave train (Figure 5a-c). For every atmospheric variable used in the study, only those regressed anomalies that are significant at 95% confidence level are displayed. The lead-lag regression analysis of winds at 300 hPa onto the PC1 shows that at day -6, there are anomalous northerly winds over western Europe reaching up to the west-central Mediterranean region and there

are anomalous southerly winds over the eastern Atlantic at around  $40^{\circ}\text{N}$  (figure not shown). These northerly wind anomalies bring anomalous cold air from the higher latitudes (Figure S2) and are associated with an anomalous high-pressure area over coastal western Europe. On day -4, with the enhancement of the upper-level high (Figure 5d) over coastal western Europe, the cold northerly wind intrusion over the west-central Mediterranean region gets further strengthened (Figure 5a). These strengthened anomalous northerly winds invades the subtropical westerly jet at its entrance region over the central Mediterranean region and form an upper-level convergence zone over the region (Figure 5g) with anomalous southerlies over the eastern Mediterranean region. Syed et al. (2006) describe this as a western disturbance. Li and Sun (2015) show that this disturbance triggers a quasi-barotropic Rossby wave which propagates zonally eastwards along the subtropical westerly jet axis, where the jet act as a Rossby waveguide.

Similar to the findings of Li and Sun (2015) we observe that by day -2, the succession of alternating northerlies and southerlies further gets established over the north Arabian Sea and the north Bay of Bengal along the subtropical westerly jet axis (figure not shown). This forms a wave train extending from the subtropical eastern Atlantic to the Indian subcontinent leading to the establishment of an anomalous cyclonic circulation over the Indian region. On day -2, the wave train along the subtropical westerly jet axis can be noticed in the regressed geopotential anomalies also with lows over the eastern Mediterranean and Indian region and highs over the western Mediterranean region and the Persian Gulf countries (figure not shown). By day 0, the wave further propagates eastwards zonally towards east Asia along the subtropical westerly jet axis and the cyclonic circulation over India becomes stronger (Figure 5b). The eastward propagation of the wave is also seen in the geopotential height anomalies (Figure 5e). It is observed that in the wave train, the convergence centers are located ahead of the anomalous high geopotential height regions and behind the anomalous low geopotential height regions (Figure 5g-h). The pattern of the wave train as seen from the meridional winds from the subtropical eastern Atlantic to the Indian region is similar to the composites of the north-northeastward moving cyclones.

Temporal-zonal sections of the meridional winds and geopotential height averaged over  $20^{\circ}\text{-}35^{\circ}\text{N}$  shows the propagation of the wave from the subtropical east Atlantic to the Indian region (Figure 6a, b). The upstream signal (over the subtropical east Atlantic and western Mediterranean region) reaches its peak 3-4 days before the peak of the wave train (day 0). It takes about 4 days for the wave train to reach up to India from the Mediterranean region and affect the wind circulation pattern over India. Also, the wave activity centers move slowly eastward with time, this eastward movement of the wave activity centers is indicated by the eastward tilting of the activity lobes (Figure 6a, b). A similar feature of the wave train is reported by Huang et al. (2020) where they show that it takes 5-6 days for the wave to travel from the eastern North Atlantic to the western North Pacific. By day 0, that is at the peak day of the

wave activity, it is seen that the anomalous high over coastal western Europe starts weakening (Figure 5e). Due to this, the southerlies and northerlies over the east Atlantic and the central Mediterranean region starts weakening. This cause a weakening of the upper-level convergence zone over the east-central Mediterranean region (Figure 5h). However, at day 0, over the Indian region, the northerlies and southerlies and the associated cyclonic circulation are the strongest. This is similar to Huang et al. (2020), in which they show that the downstream propagation of the wave along the subtropical westerly jet is associated with the dissipation of the lobes in the upstream region where the energy is initially emitted (western Mediterranean region), while the lobes in the downstream regions gradually strengthen due to the absorption of the energy. Further, it is seen that the weakening of the convergence zone over the east-central Mediterranean region which is also the subtropical westerly jet entrance region, leads to weakening of the Rossby wave activity and by day +4 this induces a break in the Rossby waveguide along the subtropical westerly jet (Figure 5c, f). The break in the Rossby waveguide leads to the weakening of the anomalous northerlies and southerlies over the Arabian Sea and the Bay of Bengal respectively and a complete dissipation of the cyclonic circulation over the Indian region by day +6 (figure not shown).

This shows that the north-northeastward moving cyclones are associated with an anomalous cyclonic circulation present over India which provides southerly steering to the cyclone. This anomalous cyclonic circulation over India is linked with an eastward-moving Rossby wave train along the subtropical westerly jet axis that propagates from subtropical east Atlantic to the Indian subcontinent and affects the wind circulation over the Indian subcontinent including the Bay of Bengal.

#### 4. Discussion and Summary

The cyclones during November in the Bay of Bengal follow two distinct tracks. Some cyclones move in a north-northeastward direction and make landfall over the West Bengal, Bangladesh, or Myanmar coasts while others move in the west-northwestward and make landfall over the Odisha, Andhra Pradesh, Tamil Nadu or Sri Lanka coasts. It is observed that the upper-level winds (300 hPa) governing these two cyclone track clusters are different from each other. During the north-northeastward moving cyclones, the westerlies penetrate more southward than normal over India and western Bay of Bengal. There are anomalous southerlies over the north and central Bay of Bengal and anomalous westerlies over the west and south Bay of Bengal. These anomalous winds over the Bay of Bengal ensue an anomalous cyclonic circulation centered over the Indian landmass. This cyclonic circulation is linked with the eastward-moving wave train along the subtropical westerly jet stream. Analysis shows that 4-5 days before the north-northeastward moving cyclone genesis, a wave train along the subtropical westerly jet is triggered by the anomalous cold northerly intrusion over the west-central Mediterranean region. The cold northerly intrusion over the Mediterranean region creates an upper-level convergence zone over the area

which is also the subtropical westerly jet entrance region. The upper-level convergence over the Mediterranean region plays an important role in exciting the wave train along the subtropical westerly jet stream with the jet acting as a waveguide (Li & Sun, 2015; Watanabe, 2004). This wave train has Rossby wave characteristics and is zonally trapped, and moves eastward with time, leading to the development of anomalous northerlies and southerlies (accompanied by anomalous low and high geopotential height) along the jet. In four days after its origin, the wave train reaches India and the adjoining Bay of Bengal with an anomalous cyclonic circulation over the Indian landmass leading to the establishment of anomalous southerlies over the north and the central Bay of Bengal and anomalous westerlies over the remaining parts of the basin. This anomalous wind pattern causes the cyclones to move in a north-northeastward direction and make landfall over the West Bengal, Bangladesh or Myanmar coasts. Figure 7 shows a schematic illustration of the sub-tropical Rossby wave affecting the track of the cyclone in the Bay of Bengal. In the case of west-northwestward moving cyclones, there is an absence of Rossby wave train along the subtropical westerly jet. As a result, there is an absence of any anomalous cyclonic circulation over the Indian landmass and anomalous easterlies prevail over the Bay of Bengal steering the cyclone in the climatological wind direction that is in west-northwestward direction and the cyclones make landfall over the Odisha, Andhra Pradesh, Tamil Nadu or Sri Lanka coasts.

Studies have shown that the North Atlantic Oscillation (NAO) also induces an eastward propagating wave train along the subtropical westerly jet axis (Miaoqing et al., 2008; Syed et al., 2006; Watanabe, 2004). This connection of the NAO to the downstream Rossby wave propagation co-occurs with the upper-level divergence over the Mediterranean Sea (Ding & Li, 2017; Watanabe, 2004). However, its connection with the circulation pattern governing the track of the cyclones in the Bay of Bengal is yet to be explored. The current study provides a new mechanism that improves our understanding on the factors controlling the tracks of cyclones in the Bay of Bengal. Improving their representation in the forecast models might be helpful in advancing the lead time of cyclone prediction. Climate models project a decrease in the frequency of cyclones making landfall at the east coast of India in the future (Bell et al., 2020). However, the mechanism controlling this projected decrease in the frequency of cyclones is not yet clear. The Bay of Bengal is surrounded by densely populated coastlines, hence, even a slight change in the tracks of cyclones can have a vast devastating socio-economic impact. It remains to be seen whether the mechanism controlling the steering winds mentioned in this study will also change in the future altering the cyclone landfall locations.

### **Conflict of Interest**

The authors declare no conflicts of interest relevant to this study.

### **Data Availability Statement**

The cyclone data is obtained from IBTrACS and is available at <https://www.ibtracs.org/>

w.ncdc.noaa.gov/ibtracs/ website. Various atmospheric variables used in the study are obtained from ERA5 reanalysis dataset and is available at <https://www.ecmwf.int/en/forecasts/datasets/reanalysis-datasets/era5> website.

## References

- Alam, M. M., Hossain, M. A., & Shafee, S. (2003). Frequency of Bay of Bengal cyclonic storms and depressions crossing different coastal zones. *International Journal of Climatology*, 23(9), 1119–1125. <https://doi.org/10.1002/joc.927>
- Balaguru, K., Leung, L. R., Lu, J., & Foltz, G. R. (2016). A meridional dipole in premonsoon bay of bengal tropical cyclone activity induced by ENSO. *Journal of Geophysical Research*, 121(12), 6954–6968. <https://doi.org/10.1002/2016JD024936>
- Bell, S. S., Chand, S. S., Tory, K. J., Ye, H., & Turville, C. (2020). North Indian Ocean tropical cyclone activity in CMIP5 experiments: Future projections using a model-independent detection and tracking scheme. *International Journal of Climatology*, (April), 1–14. <https://doi.org/10.1002/joc.6594>
- Bhardwaj, P., Pattanaik, D. R., & Singh, O. (2019). Tropical cyclone activity over Bay of Bengal in relation to El Niño-Southern Oscillation. *International Journal of Climatology*, 39(14), 5452–5469. <https://doi.org/10.1002/joc.6165>
- Biswas, H. R., & Kundu, P. K. (2018). A principal component analysis based model to predict post-monsoon tropical cyclone activity in the Bay of Bengal using oceanic Niño index and dipole mode index. *International Journal of Climatology*, 38(5), 2415–2422. <https://doi.org/10.1002/joc.5344>
- Bo-Tao, Z. (2013). Weakening of Winter North Atlantic Oscillation Signal in Spring Precipitation over Southern China. *Atmospheric and Oceanic Science Letters*, 6(5), 248–252. <https://doi.org/10.3878/j.issn.1674-2834.13.0010>
- Branstator, G. (2002). Circumglobal teleconnections, the jet stream waveguide, and the North Atlantic Oscillation. *Journal of Climate*, 15(14), 1893–1910. [https://doi.org/10.1175/1520-0442\(2002\)015<1893:CTTJSW>2.0.CO;2](https://doi.org/10.1175/1520-0442(2002)015<1893:CTTJSW>2.0.CO;2)
- Chan, Johnny C.L. (2005, January 12). The physics of tropical cyclone motion. *Annual Review of Fluid Mechanics*. Annual Reviews Inc. <https://doi.org/10.1146/annurev.fluid.37.061903.175702>
- Chan, Johny C. L., & Gray, W. M. (1982). Tropical Cyclone Movement and Surrounding Flow Relationships. *Monthly Weather Review*, 110(10), 1354–1374.
- Chan, Johny C. L., & Williams, R. T. (1987). Analytical and Numerical Studies of the Beta-Effect in Tropical Cyclone Motion. Part I: Zero Mean Flow. *Journal of the Atmospheric Sciences*, 44(9), 1257–1265.
- Chen, T. C., Wang, S. Y., Yen, M. C., & Clark, A. J. (2009). Impact of the intraseasonal variability of the western North-Pacific large-scale circulation on tropical cyclone tracks. *Weather and Forecasting*, 24(3), 646–666. <https://doi.org/10.1175/2008WAF2222186.1>
- Chittibabu, P., Dube, S. K., Macnabb, J. B., Murty, T. S., Rao, A. D., Mohanty, U. C., & Sinha, P. C. (2004). Mitigation of flooding and cyclone hazard in Orissa, India. *Natural Hazards*, 31(2), 455–485. <https://doi.org/10.1023/B:NHAZ.0000023362.26409.22>
- Ding, F., & Li, C. (2017). Subtropical westerly jet waveguide and winter persistent heavy rainfall in south China. *Journal of Geophysical Research*, 122(14), 7385–7400. <https://doi.org/10.1002/2017jd026530>
- Ding, Q., & Wang, B. (2007). Intraseasonal teleconnection between the sum-

mer Eurasian wave train and the Indian Monsoon. *Journal of Climate*, 20(15), 3751–3767. <https://doi.org/10.1175/JCLI4221.1>

Elsner, J. B. (2003). Tracking hurricanes. *Bulletin of the American Meteorological Society*, 84(3), 353–356. <https://doi.org/10.1175/BAMS-84-3-353>

Felton, C. S., Subrahmanyam, B., & Murty, V. S. N. (2013). ENSO-modulated cyclogenesis over the Bay of Bengal. *Journal of Climate*, 26(24), 9806–9818. <https://doi.org/10.1175/JCLI-D-13-00134.1>

Galarneau, T. J., & Davis, C. A. (2013). Diagnosing forecast errors in tropical cyclone motion. *Monthly Weather Review*, 141(2), 405–430. <https://doi.org/10.1175/MWR-D-12-00071.1>

George, J. E., & Gray, W. M. (1976). Tropical Cyclone Motion and Surrounding Parameter Relationships. *Journal of Applied Meteorology*, 15(12), 1252–1264. [https://doi.org/10.1175/1520-0450\(1976\)015<1252:TCMASP>2.0.CO;2](https://doi.org/10.1175/1520-0450(1976)015<1252:TCMASP>2.0.CO;2)

Girishkumar, M. S., & Ravichandran, M. (2012). The influences of ENSO on tropical cyclone activity in the Bay of Bengal during October–December. *Journal of Geophysical Research: Oceans*, 117(2), 1–13. <https://doi.org/10.1029/2011JC007417>

Girishkumar, M. S., Suprit, K., Vishnu, S., Prakash, V. P. T., & Ravichandran, M. (2015). The role of ENSO and MJO on rapid intensification of tropical cyclones in the Bay of Bengal during October–December. *Theoretical and Applied Climatology*, 120(3–4), 797–810. <https://doi.org/10.1007/s00704-014-1214-z>

Harr, P. A., & Elsberry, R. L. (1991). Tropical Cyclone Track Characteristics as a Function of Large-Scale Circulation Anomalies. *Monthly Weather Review*, 119(6), 1448–1468.

Ho, C. H., Baik, J. J., Kim, J. H., Gong, D. Y., & Sui, C. H. (2004). Interdecadal changes in summertime typhoon tracks. *Journal of Climate*, 17(9), 1767–1776. [https://doi.org/10.1175/1520-0442\(2004\)017<1767:ICISTT>2.0.CO;2](https://doi.org/10.1175/1520-0442(2004)017<1767:ICISTT>2.0.CO;2)

Holland, G. J. (1983). Tropical Cyclone Motion: Environmental Interaction Plus a Beta Effect. *Journal of the Atmospheric Sciences*. [https://doi.org/10.1175/1520-0469\(1983\)040<0328:TCMEIP>2.0.CO;2](https://doi.org/10.1175/1520-0469(1983)040<0328:TCMEIP>2.0.CO;2)

Hoskins, B. J., & Ambrizzi, T. (1993). Rossby Wave Propagation on a Realistic Longitudinally Varying Flow. *Journal of Atmospheric Science*, 50, 1661–1671. [https://doi.org/10.1175/1520-0469\(1993\)050<1661:RWPOAR>2.0.CO;2](https://doi.org/10.1175/1520-0469(1993)050<1661:RWPOAR>2.0.CO;2)

Hu, K., Huang, G., Wu, R., & Wang, L. (2018). Structure and dynamics of a wave train along the wintertime Asian jet and its impact on East Asian climate. *Climate Dynamics*, 51(11–12), 4123–4137. <https://doi.org/10.1007/s00382-017-3674-1>

Huang, S., Li, X., & Wen, Z. (2020). Characteristics and possible sources of the intraseasonal South Asian jet wave train in boreal winter. *Journal of Climate*, 33(24), 10523–10537. <https://doi.org/10.1175/JCLI-D-20-0125.1>

Hunt, K. M.R., Curio, J., Turner, A. G., & Schiemann, R. (2018a). Subtropical Westerly Jet Influence on Occurrence of Western Disturbances and Tibetan Plateau Vortices. *Geophysical Research Letters*, 45(16), 8629–8636. <https://doi.org/10.1029/2018GL077734>

Hunt, Kieran M.R., Turner, A. G., & Shaffrey, L. C. (2018b). The evolution, seasonality and impacts of western disturbances. *Quarterly Journal of the Royal Meteorological Society*, 144(710), 278–290. <https://doi.org/10.1002/qj.3200>

Kikuchi, K., Wang, B., & Fudeyasu, H. (2009). Genesis of tropical cyclone Nargis revealed by multiple satellite observations. *Geophysical Research Letters*, 36(6). <https://doi.org/10.1029/2009GL037296>

Knapp, K. R., Kruk, M. C., Levinson,

D. H., Diamond, H. J., & Neumann, C. J. (2010). The International Best Track Archive for Climate Stewardship (IBTrACS). *Bulletin of the American Meteorological Society*, 91(3), 363–376. <https://doi.org/10.1175/2009BAMS2755.1Ko>, K. C., & Hsu, H. H. (2006). Sub-monthly circulation features associated with tropical cyclone tracks over the East Asian Monsoon area during July-August season. *Journal of the Meteorological Society of Japan*, 84(5), 871–889. <https://doi.org/10.2151/jmsj.84.871Kossin>, J. P., Camargo, S. J., & Sitkowski, M. (2010). Climate modulation of north atlantic hurricane tracks. *Journal of Climate*, 23(11), 3057–3076. <https://doi.org/10.1175/2010JCLI3497.1Krishnamohan>, K. S., Mohanakumar, K., & Joseph, P. V. (2012). The influence of Madden-Julian Oscillation in the genesis of North Indian Ocean tropical cyclones. *Theoretical and Applied Climatology*, 109(1–2), 271–282. <https://doi.org/10.1007/s00704-011-0582-xKuang>, X., & Zhang, Y. (2005). Seasonal Variation of the East Asian Subtropical Westerly Jet and Its Association with the Heating Field over East Asia. *ADVANCES IN ATMOSPHERIC SCIENCES*, 22(6), 831–840.Landsea, C. W. (2005). Hurricanes and global warming. *Nature*, 438(7071), E11–E12.Li, C., & Sun, J. (2015). Role of the subtropical westerly jet waveguide in a southern China heavy rainstorm in December 2013. *Advances in Atmospheric Sciences*, 32(5), 601–612. <https://doi.org/10.1007/s00376-014-4099-yLi>, D., Chen, H., Liu, P., & Zhou, C. (2020). Zonally asymmetric mode of anomalous activity in summer Asian subtropical westerly jet and its possible sources. *Theoretical and Applied Climatology*, 139(1–2), 17–32. <https://doi.org/10.1007/s00704-019-02934-5Li>, X., Chen, Y. D., & Zhou, W. (2017a). Response of winter moisture circulation to the India-Burma trough and its modulation by the South Asian waveguide. *Journal of Climate*, 30(4), 1197–1210. <https://doi.org/10.1175/JCLI-D-16-0111.1Li>, X., Chen, Y. D., & Zhou, W. (2017b). Response of winter moisture circulation to the India-Burma trough and its modulation by the South Asian waveguide. *Journal of Climate*, 30(4), 1197–1210. <https://doi.org/10.1175/JCLI-D-16-0111.1Li>, Z., Yu, W., Li, T., Murty, V. S. N., & Tangang, F. (2013). Bimodal character of cyclone climatology in the Bay of Bengal modulated by monsoon seasonal cycle. *Journal of Climate*, 26(3), 1033–1046. <https://doi.org/10.1175/JCLI-D-11-00627.1Lin>, I. I., Chen, C. H., Pun, I. F., Liu, W. T., & Wu, C. C. (2009). Warm ocean anomaly, air sea fluxes, and the rapid intensification of tropical cyclone Nargis (2008). *Geophysical Research Letters*, 36(3). <https://doi.org/10.1029/2008GL035815Liu>, K. S., & Chan, J. C. L. (2008). Interdecadal variability of western North Pacific tropical cyclone tracks. *Journal of Climate*, 21(17), 4464–4476. <https://doi.org/10.1175/2008JCLI2207.1Madsen>, H., & Jakobsen, F. (2004). Cyclone induced storm surge and flood forecasting in the northern Bay of Bengal. *Coastal Engineering*, 51(4), 277–296. <https://doi.org/10.1016/j.coastaleng.2004.03.001Mahala>, B. K., Nayak, B. K., & Mohanty, P. K. (2015). Impacts of ENSO and IOD on tropical cyclone activity in the Bay of Bengal. *Natural Hazards*, 75(2), 1105–1125. <https://doi.org/10.1007/s11069-014-1360-8Mei>, W., Xie, S. P., & Zhao, M.

(2014). Variability of tropical cyclone track density in the North Atlantic: Observations and high-resolution simulations. *Journal of Climate*, 27(13), 4797–4814. <https://doi.org/10.1175/JCLI-D-13-00587.1>Miaoqing, S., Yihui, D., & Zunya, W. (2008). Relationship Between Rossby Wave Propagation in Southern Branch of Westerlies and the Formation of the Southern Branch Trough in Wintertime. *Journal of Applied Meteorological Science*, 19(6), 731–740.Mohapatra, M., & Vijay Kumar, V. (2017). Interannual variation of tropical cyclone energy metrics over North Indian Ocean. *Climate Dynamics*, 48(5–6), 1431–1445. <https://doi.org/10.1007/s00382-016-3150-3>Neumann, C. J. (1993). *Global overview. Chapter 1, Global guide to tropical cyclone forecasting*. Geneva.Ng, E. K. W., & Chan, J. C. L. (2012). Interannual variations of tropical cyclone activity over the north Indian Ocean. *International Journal of Climatology*, 32(6), 819–830. <https://doi.org/10.1002/joc.2304>Pattanaik, D. R., & Rama Rao, Y. V. (2009). Track prediction of very severe cyclone “Nargis” using high resolution weather research forecasting (WRF) model. *Journal of Earth System Science*, 118(4), 309–329. <https://doi.org/10.1007/s12040-009-0031-8>Ren, X., Yang, D., & Yang, X. Q. (2015). Characteristics and mechanisms of the subseasonal eastward extension of the South Asian high. *Journal of Climate*, 28(17), 6799–6822. <https://doi.org/10.1175/JCLI-D-14-00682.1>Sahoo, B., & Bhaskaran, P. K. (2016). Assessment on historical cyclone tracks in the Bay of Bengal, east coast of India. *International Journal of Climatology*, 36(1), 95–109. <https://doi.org/10.1002/joc.4331>Singh, K., Panda, J., Sahoo, M., & Mohapatra, M. (2019). Variability in Tropical Cyclone Climatology over North Indian Ocean during the Period 1891 to 2015. *Asia-Pacific Journal of Atmospheric Sciences*, 55(2), 269–287. <https://doi.org/10.1007/s13143-018-0069-0>Singh, V.K., Roxy, M. K., & Deshpande, M. (2020). The unusual long track and rapid intensification of very severe cyclone Ockhi. *Current Science*, 119(5), 771–779.Singh, Vineet Kumar, & Roxy, M. K. (2020). A review of the ocean-atmosphere interactions during tropical cyclones in the north Indian Ocean. *ArXiv Preprint ArXiv:2012.04384*.Singh, Vineet Kumar, Roxy, M. K., & Deshpande, M. (2021). Role of warm ocean conditions and the MJO in the genesis and intensification of extremely severe cyclone Fani. *Scientific Reports*, 11(1), 3607. <https://doi.org/10.1038/s41598-021-82680-9>Song, J., Li, C., & Zhou, W. (2014). High and low latitude types of the downstream influences of the North Atlantic Oscillation. *Climate Dynamics*, 42(3–4), 1097–1111. <https://doi.org/10.1007/s00382-013-1844-3>Srinivasan, V., & Ramamurthy, K. (1973). *Forecasting manual, part IV:Comprehensive articles on selected topics, FMU Rep. IV-10*. New Delhi.Sun, J., Ming, J., Zhang, M., & Yu, S. (2018). Circulation Features Associated with the Record-Breaking Rainfall over South China in June 2017. *Journal of Climate*, 31(18), 7209–7224. <https://doi.org/10.1175/JCLI-D-17-0903.1>Syed, F. S., Giorgi, F., Pal, J. S., & King, M. P. (2006). Effect of remote forcings on the winter precipitation of central southwest Asia part 1: Observations. *Theoretical and Applied Climatology*, 86(1–4), 147–160. <https://doi.org/10.1007/s00704-005-0217-1>Wang, B., Elsberry, R. L., Yuqing, W., & Liguang, W. (1998). Dynamics in Tropical Cyclone Motion: A Review. *Chinese Journal of Atmospheric Sciences*. Retrieved from

[http://www.soest.hawaii.edu/users/bwang/bw/pubs/after57/22\\_535.html](http://www.soest.hawaii.edu/users/bwang/bw/pubs/after57/22_535.html) Watanabe, M. (2004). Asian jet waveguide and a downstream extension of the North Atlantic Oscillation. *Journal of Climate*, 17(24), 4674–4691. <https://doi.org/10.1175/JCLI-3228.1> Wen, M., Yang, S., Kumar, A., & Zhang, P. (2009). An analysis of the large-scale climate anomalies associated with the snowstorms affecting China in January 2008. *Monthly Weather Review*, 137(3), 1111–1131. <https://doi.org/10.1175/2008MWR2638.1> Williams, R. T., & Chan, J. C. L. (1994). Numerical studies of the beta effect in tropical cyclone motion. Part II: Zonal mean flow effects. *Journal of Atmospheric Sciences*, 51(8), 1065–1076. [https://doi.org/10.1175/1520-0469\(1994\)051<1065:NSOTBE>2.0.CO;2](https://doi.org/10.1175/1520-0469(1994)051<1065:NSOTBE>2.0.CO;2) Wirth, V., Riemer, M., Chang, E. K. M., & Martius, O. (2018). Rossby Wave Packets on the Midlatitude Waveguide—A Review. *Monthly Weather Review*, 146(7), 1965–2001. <https://doi.org/10.1175/MWR-D-16-0483.1> WMO. (2021). *State of the Global Climate 2020*. Geneva. Retrieved from [https://library.wmo.int/index.php?lvl=notice\\_display&id=21880#.YJL](https://library.wmo.int/index.php?lvl=notice_display&id=21880#.YJL) L., & Wang, B. (2004). Assessing Impacts of Global Warming on Tropical Cyclone Tracks. *Journal of Climate*, 17(8), 1686–1699. [https://doi.org/10.1175/1520-0442\(2004\)017<1686:AIOGWO>2.0.CO;2](https://doi.org/10.1175/1520-0442(2004)017<1686:AIOGWO>2.0.CO;2) Wu, Liguang, Wang, B., & Geng, S. (2005). Growing typhoon influence on east Asia. *Geophysical Research Letters*, 32(18), 1–4. <https://doi.org/10.1029/2005GL022937> Wu, Q., Wang, X., & Tao, L. (2020). Interannual and interdecadal impact of Western North Pacific Subtropical High on tropical cyclone activity. *Climate Dynamics*, 54(3–4), 2237–2248. <https://doi.org/10.1007/s00382-019-05110-7> Xie, L., Yan, T., Pietrafesa, L. J., Morrison, J. M., & Karl, T. (2005). Climatology and interannual variability of North Atlantic hurricane tracks. *Journal of Climate*, 18(24), 5370–5381. <https://doi.org/10.1175/JCLI3560.1> Xiuzhen, L., & Zhou, W. (2016). Modulation of the interannual variation of the India-Burma Trough on the winter moisture supply over Southwest China. *Climate Dynamics*, 46(1–2), 147–158. <https://doi.org/10.1007/s00382-015-2575-4> Yanase, W., Taniguchi, H., & Satoh, M. (2010). The genesis of tropical cyclone Nargis (2008): Environmental modulation and numerical predictability. *Journal of the Meteorological Society of Japan*, 88(3), 497–519. <https://doi.org/10.2151/jmsj.2010-314> Yang, S., Lau, K. M., Yoo, S. H., Kinter, J. L., Miyakoda, K., & Ho, C. H. (2004). Upstream subtropical signals preceding the Asian summer monsoon circulation. *Journal of Climate*, 17(21), 4213–4229. <https://doi.org/10.1175/JCLI3192.1> Yonekura, E., & Hall, T. M. (2014). ENSO effect on East Asian tropical cyclone landfall via changes in tracks and genesis in a statistical model. *Journal of Applied Meteorology and Climatology*, 53(2), 406–420. <https://doi.org/10.1175/JAMC-D-12-0240.1> Yuan, J. P., & Cao, J. (2013). North Indian Ocean tropical cyclone activities influenced by the Indian Ocean Dipole mode. *Science China Earth Sciences*, 56(5), 855–865. <https://doi.org/10.1007/s11430-012-4559-0> Yun, K. S., Chan, J. C. L., & Ha, K. J. (2012). Effects of SST magnitude and gradient on typhoon tracks around East Asia: A case study for Typhoon Maemi (2003). *Atmospheric Research*, 109–110, 36–51. <https://doi.org/10.1016/j.atmosres.2012.02.012> Zhang, W., Graf, H. F., Leung, Y., & Herzog, M. (2012). Different El Niño types

and tropical cyclone landfall in East Asia. *Journal of Climate*, 25(19), 6510–6523. <https://doi.org/10.1175/JCLI-D-11-00488.1> Zhang, W., Leung, Y., & Chan, J. C. L. (2013). The analysis of tropical cyclone tracks in the western north pacific through data mining. Part i: Tropical cyclone recurvature. *Journal of Applied Meteorology and Climatology*, 52(6), 1394–1416. <https://doi.org/10.1175/JAMC-D-12-045.1> Zhou, W., Chan, J. C. L., Chen, W., Ling, J., Pinto, J. G., & Shao, Y. (2009). Synoptic-scale controls of persistent low temperature and icy weather over Southern China in January 2008. *Monthly Weather Review*, 137(11), 3978–3991. <https://doi.org/10.1175/2009MWR2952.1>

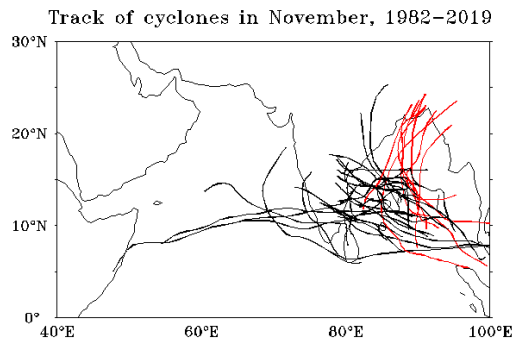


Figure 1. Track of cyclones in November during the period 1982–2019. The tracks in black color denote the cyclones that move west-northwestward and make landfall over Sri Lanka, Tamil Nadu, Andhra Pradesh or Odisha coasts. The tracks in red color denotes the cyclones that move north-northeastward and make landfall at West Bengal, Bangladesh or Myanmar coasts.

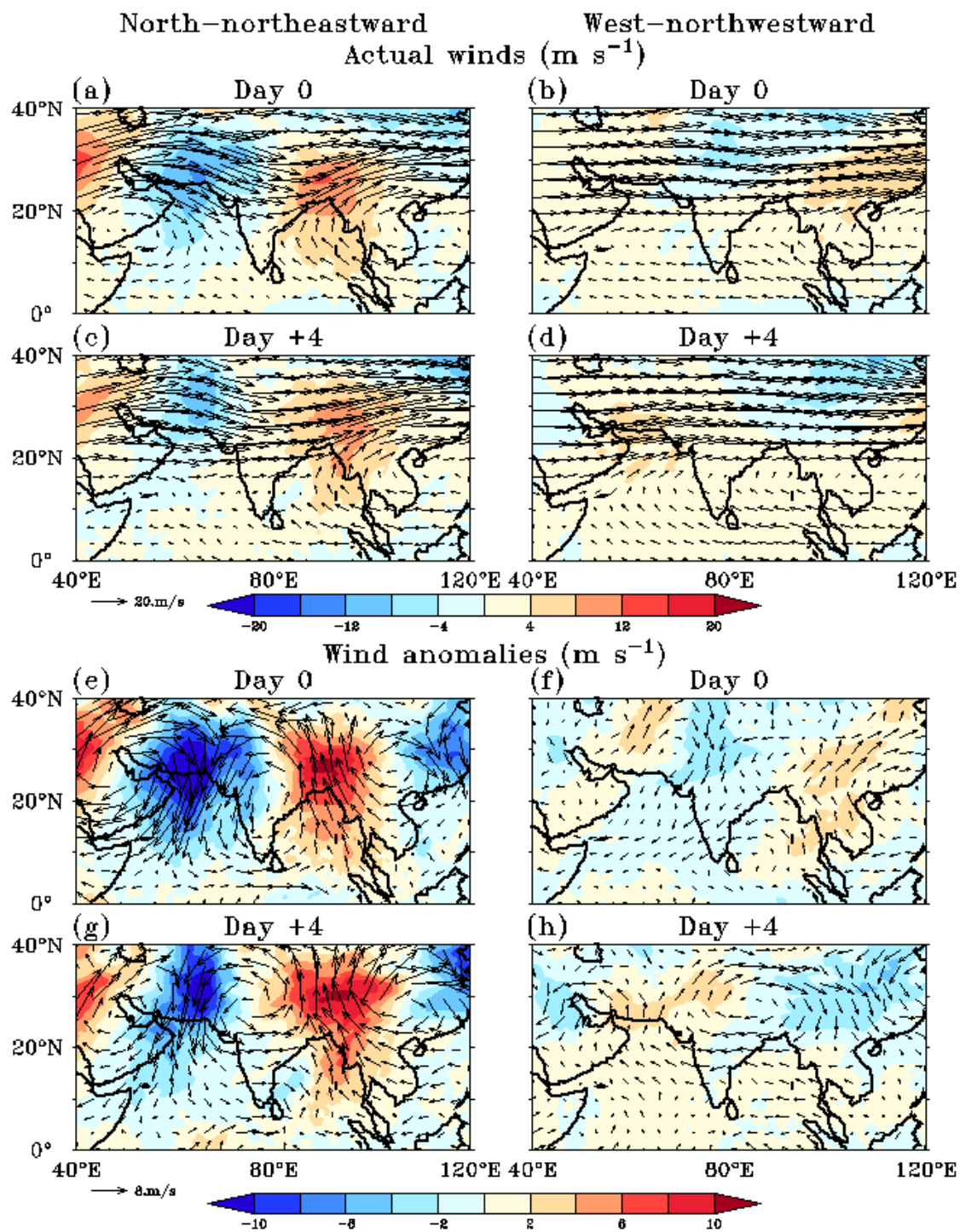


Figure 2. Composite evolution of upper-level (300 hPa) winds ( $\text{m s}^{-1}$ , vector) and meridional winds ( $\text{m s}^{-1}$ , color) with the cyclone vortex removed, for the north-northeastward moving cyclones (left column) and west-northwestward moving cyclones (right column) for (a-b) day 0 (c-d) day +4 after cyclone genesis. (e-h) Same as (a-d) but for wind ( $\text{m s}^{-1}$ ) and meridional wind anomalies ( $\text{m s}^{-1}$ , color).

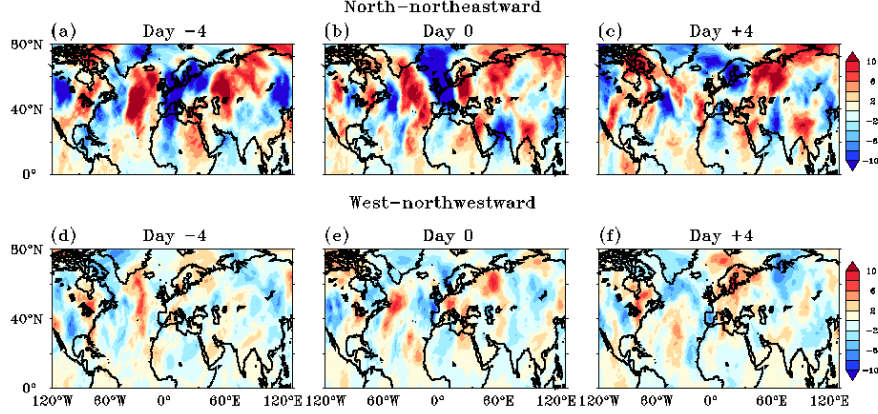


Figure 3. Composite evolution of upper level (300 hPa) meridional wind anomalies ( $\text{m s}^{-1}$ , color) for the (a-c) north-northeastward moving cyclones (d-f) west-northwestward moving cyclones. Red color denotes southerly wind anomalies and blue color denotes northerly wind anomalies.

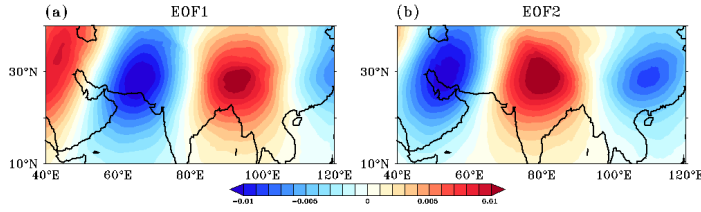


Figure 4. Spatial distributions of the (a) first and (b) second EOF modes of daily meridional wind anomaly ( $\text{m s}^{-1}$ , color) at 300 hPa in November during

the period 1982–2019.

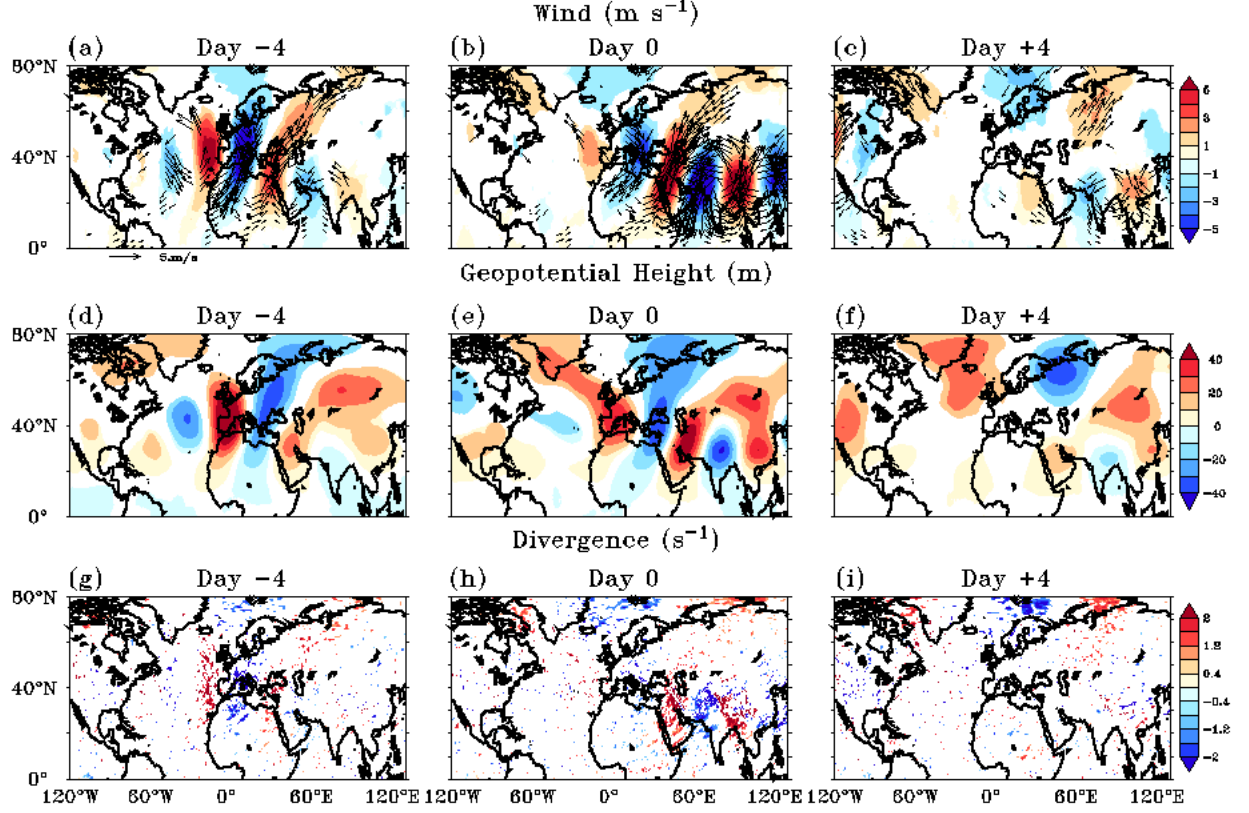


Figure 5. Lead-lag regression of (a-c) wind ( $\text{m s}^{-1}$ , vector) and meridional wind ( $\text{m s}^{-1}$ , color) (d-f) Geopotential height (m, color) (g-i) Divergence ( $10^6 \text{ s}^{-1}$ , color) anomalies on the PC1. Only those anomalies are shown which are significant at 95% confidence level.

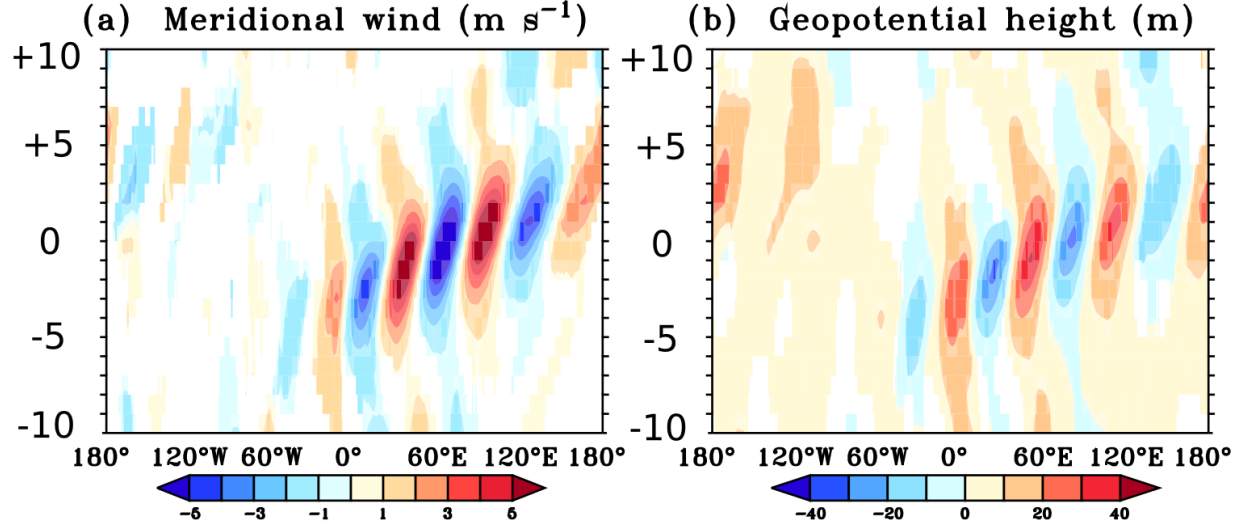


Figure 6. Temporal-zonal sections of anomalies of (a) meridional wind ( $\text{m s}^{-1}$ ) (b) geopotential height (m) regressed with PC1, averaged over  $20^{\circ}$ - $35^{\circ}$ N from day -10 to day +10. Only those anomalies are shown which are significant at 95% confidence level.

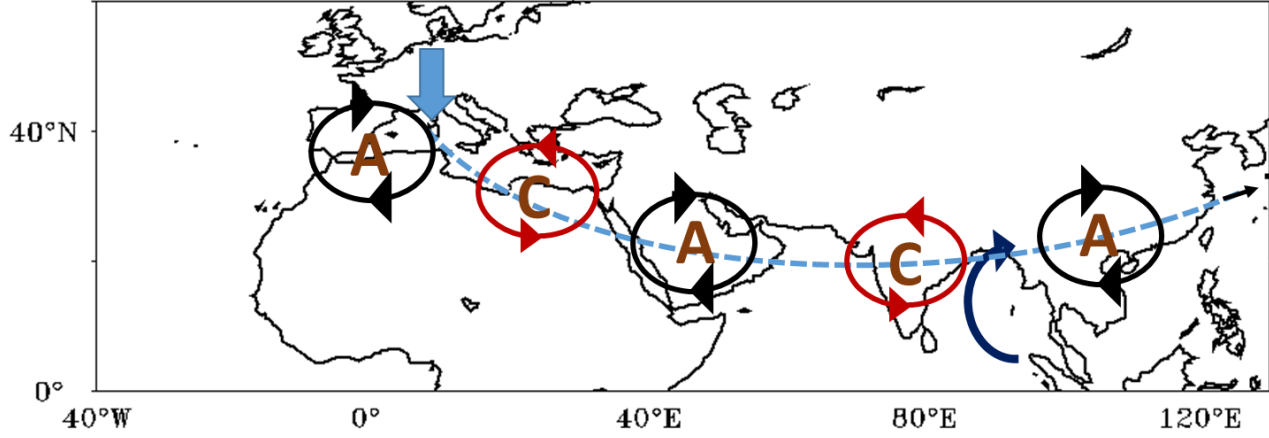


Figure 7. Schematic illustration of the sub-tropical Rossby wave guiding the north-northeastward moving cyclones in the Bay of Bengal. The blue arrow represent the cold northerly intrusion over the Mediterranean region. Letter A represent the upper level anticyclonic wind anomaly and letter B represent the upper level cyclonic wind anomaly. The dash blue line from the Mediterranean region to the east China passing through Indian subcontinent denotes the direction of propagation of the Rossby wave. Thick solid line arrow over the Bay of Bengal represents the direction of movement of the cyclone.